MULTIMODE AND RESONANCE EFFECTS IN TRANSVERSE BEAM BLOW-UP†

R. L. Gluckstern and S. C. Prasad
University of Massachusetts, Amherst

ABSTRACT

The usual estimate of the current at which transverse beam blow-up occurs is made under the assumption of a single transverse mode not in resonance with the beam frequency. For a single mode the starting current decreases by less than a factor of two at resonance. We have treated the case of several modes numerically, using an eigen-mode method, and find considerable structure in the dependence of the starting current on the frequency of the transverse band. Specifically we find reductions of up to a factor two as the frequencies of the main mode and the adjacent modes pass through resonance with the beam frequency. Furthermore, there are additional variations exactly midway between these resonances. Typical numerical results of this eigen-mode method are presented. In addition, the particular features of each anomaly are derived from an analysis of which modes are most important at each frequency. Our analysis and results once again confirm the fact that the starting current never decreases below half of the value for a single non-resonant mode.

I. Introduction

In previous work[1,2] the interaction of a bunched beam with a standing wave linac cavity was analyzed in terms of the amplitudes of the various resonant transverse modes of the cavity. Difference equations were derived for the change in these amplitudes with each beam pulse. A limit to the current is set by the requirement that the solution of these equations should not contain a runaway component. This was explored numerically[1] where it was found neglect of all but a single mode gave a reasonable approximation to the results with several modes. The calculations were repeated with greater accuracy[2] by obtaining the eigenvalues of the homogeneous difference equations and the results were approximately the same. In the present work the effect of resonances between the frequencies of the cavity modes and multiples of the beam pulse frequency was explored, yielding a rather elaborate structure for the dependence of the starting current on the frequency of transverse bands in the vicinity of these resonances. The details of this structure are explained, but the previous result still appears to be valid: The starting current is reduced by at most a factor of two compared with the result for a single non-resonant mode.

II. Difference Equation

The difference equation for $H_j^{(m)}$, the field amplitude of the j^{th} mode after the passage of the m^{th} beam pulse through the cavity, is[2]

$$H_j^{(m+1)} e^{i\theta_j} - H_j^{(m)} = -\varepsilon_j H_j^{(m)} + \sum_k S_k [W_{jk} H_k^{(m)} - \bar{W}_{jk} H_k^{(m)*}] \quad (1)$$

where the parameters are defined in references 1 and 2. The parameter S_k is proportional to the current, ε_j is the fractional decrease in field amplitude due to r-f losses from one beam pulse to the next, $\theta_j = \omega_j \Delta t$ is a measure of the resonance between the j^{th} mode and the beam pulse frequency, $1/\Delta t$, and W_{jk}, $\bar{W}_{jk}$ are dimensionless parameters depending on α_j and α_k, the slip of the j^{th} and k^{th} modes with respect to the beam bunch.

The solution of Equation (1) can be found by setting $H_j^{(m)} = H_j \lambda^m$ and solving the resulting secular determinant for λ. If we assume that ε and S are nearly the same for all modes, one has

$$\begin{vmatrix} 1-\varepsilon+SW_{11}-\lambda e^{-i\theta_1} & -S\bar{W}_{11} & SW_{12} & -S\bar{W}_{12} & \cdots \\ -S\bar{W}^*_{11} & 1-\varepsilon+SW^*_{11}-\lambda e^{i\theta_1} & -S\bar{W}^*_{12} & SW^*_{12} & \cdots \\ SW_{21} & -S\bar{W}_{21} & 1-\varepsilon+SW_{22}-\lambda e^{-i\theta_2} & -S\bar{W}_{22} & \cdots \\ -SW^*_{21} & SW^*_{21} & -S\bar{W}^*_{22} & 1-\varepsilon+SW^*_{22}-\lambda e^{i\theta_2} & \cdots \\ \cdots & \cdots & \cdots & \cdots & \cdots \end{vmatrix} = 0 \qquad (2)$$

The starting current is then that value of S which makes the largest value of $|\lambda|$ equal to 1. Above this value of S the solution of (1) will have an exponentially growing component, corresponding to a runaway solution.

In general the largest $|\lambda|$ occurs for the mode, j, where the slip α_j, of the wave behind the beam bunch, is approximately π as the cavity is transversed. The neighboring modes exert diminishing influence on the starting current. For this reason, numerical solutions to Equation (2) have been obtained for a given set of parameters assuming that only a finite number of modes, centered at the mode with slip approximately π, contributes. The number of modes is then taken as 1, 3, 5, ... until it becomes clear that the dependence of starting current on other parameters is insensitive to the choice of the number of modes.

III. Numerical Results

We have explored a typical case for which resonance effects are expected to be important. The cavity is taken to have 40 cells, an accelerating mode of 800 Mc, and a beam bunch frequency of 200 Mc. Numerical studies are then made for the dependence of S (starting current) on the width and location of the transverse band (assumed to be near 1200 Mc which is the 6th harmonic of the beam bunch frequency). The loss parameter ε is taken to be 10^{-3}.

Figure 1 shows the variation of S with the central frequency of transverse band for a band width of 20 Mc, where we have taken into consideration 1, 3, and 5 modes. It is clear from the curves that the inclusion of several modes introduces considerably more structure into the dependence of S on the frequency of the transverse band. This will be interpreted in the next section in terms of resonances between the various modes and the beam bunch frequency.

Figure 2 gives the corresponding results for a band width of 10 Mc. One notices a strong similarity in structure to the results in Figure 1, but here the features are compressed in frequency by a factor of 2 compared with Figure 1. Computations for other band widths also show the same structure, spread by an amount proportional to the band width.

The trends in the curves indicate that only minor changes (less than a few percent) will be introduced by including additional modes. The reason for this will also be clear in the next section.

IV. Analysis of Results

It is possible to understand the structure in Figures 1 and 2 in terms of resonances with the beam bunch frequency for one or another of the contributing modes. We shall first consider the effect of a single mode and then modify the results because of the contribution of one or another of the modes in the secular determinant of Equation (2).

A. Single Mode - no resonance

It is clear that, for ε and S each of similar small magnitude ($\sim 10^{-3}$ in our present considerations), the roots of Equation (2) will also be distinct as long as each of the θ_j is not also similarly small. In fact these roots are given to order ε^2 by

$$\lambda_j \simeq e^{i\theta_j}(1 - \varepsilon + SW_{jj}), \qquad (3)$$

and the largest value of S (for which

$|\lambda| = 1$) is that given by

$$S_{max} \simeq \frac{\varepsilon}{U_{jj}} \qquad (4)$$

where U_{jk} and V_{jk} are the real and imaginary part of W_{jk}. The result in Eq. (4) is then expected to be valid as long as the values of θ_j are not small, i.e. as long as there is no resonance.

It is clear from Equation (4) that the lowest S_{max} corresponds to the highest U_{jj} which occurs, as previously mentioned, for a slip of approximately π (this is similar to the result for a traveling wave amplifier, as pointed out by P. B. Wilson[3]). For our numerical value, this corresponds to mode 61.

B. Single mode - resonance

If there is resonance between this mode and the beam bunch frequency, θ_j will be small and the root corresponding to Equation (3) comes from the 2x2 subdeterminant of Eq. (2), namely

$$\begin{vmatrix} 1-\varepsilon+SW_{11}-\lambda e^{-i\theta_1} & S\bar{W}_{11} \\ -S\bar{W}^*_{11} & 1-\varepsilon+SW^*_{11}-\lambda e^{i\theta_1} \end{vmatrix} = 0 \qquad (5)$$

or

$$\lambda = \mathrm{Re}[e^{i\theta_1}(1-\varepsilon+SW_{11})] \pm \sqrt{S^2|\bar{W}_{11}|^2-\{\mathrm{Im}[e^{i\theta_1}(1-\varepsilon+SW_{11})]\}^2}. \qquad (6)$$

For small θ_1, one writes for the root with largest $|\lambda|$

$$|\lambda| \simeq 1 - \varepsilon + SU_{11} + \mathrm{Re}\sqrt{S^2|\bar{W}_{11}|^2 - (\theta_1 + SV_{11})^2}. \qquad (7)$$

The dependence of S_{max} on θ_1 corresponds to setting $|\lambda| = 1$. The result is a combination of an ellipse and the straight line of Equation (4), whichever produces a lower S_{max}. In fact the lowest S_{max} can be seen from Equation (6) to be that corresponding to a purely real value of the quantity in square brackets, and is

$$S_{max} \simeq \frac{\varepsilon}{U_{11} + |\bar{W}_{11}|} \quad (\text{small } \theta_1) \qquad (8)$$

One can further simplify the appearance of these results by using approximate values of W. For our choice of parameters, one has

$$\alpha_j = \pi[j - 60] - 5\theta_j \qquad (9)$$

In the vicinity of resonance, θ_j is of order ε, so that all the α_j are very close to multiples of π. We will set these α's to be exactly multiples of π and will take j=61 to be the central mode, j=60, 62 to be the nearest modes, j=59, 63 to be the next nearest modes, etc. As a further simplification in notation we will designate modes 59, 60, 61, 62, 63 by the subscripts -1,0, 1,2,3, as we have already done in Equations (5)-(7).

Using these approximations, one finds $U_{11} \simeq 1$, $V_{11} \simeq 0$, $|\bar{W}_{11}| \simeq \pi/4$. Equation (7) then yields

$$\frac{S_{max}}{\varepsilon} \simeq \begin{cases} \dfrac{1-[(\pi/4)^2-(\theta_1/\varepsilon)^2(1-(\pi/4)^2)]^{1/2}}{1-(\pi/4)^2}, \\ \qquad \text{for } |\theta_1/\varepsilon| \le \pi/4 \\ 1, \quad \text{for } |\theta_1/\varepsilon| \ge \pi/4 \end{cases} \qquad (10)$$

Equation (10) corresponds to region I on the upper curve in Figures 1,2, and this resonance is clearly the explanation of the structure in this region.

A single mode resonance also exists when $\theta_{-1} \simeq 0$, $\theta_0 \simeq 0$, $\theta_2 \simeq 0$, $\theta_3 \simeq 0$ etc. However, the only one for which the corresponding S_{max} is less than $\varepsilon/U_{11} \simeq \varepsilon$ is mode 60, for which we have $U_{oo} \simeq 0$, $V_{oo} \simeq -\pi^3/24$, $|\bar{W}_{oo}| \simeq \pi^3/24$. This leads to

$$\frac{S_{max}}{\varepsilon} \simeq \frac{12}{\pi^3}\left[\frac{1 + (\theta_o/\varepsilon)^2}{(\theta_o/\varepsilon)}\right] \text{ or } 1 \qquad (11)$$

whichever is lower. This is plotted as the upper curve in region II and is clearly the explanation for the structure in this region. Note that this structure does not occur unless mode 60 is included in the numerical studies.

C. Double mode resonances

The remaining structure corresponds to an interaction between a pair of modes and the beam. In particular, the roots of the secular determinant in Equation (2) will depart from the single mode values if combinations such as $\theta_1 + \theta_j$

are of order ε. In this case the roots are given by the 2 x 2 sub-determinant

$$\begin{vmatrix} 1-\varepsilon+SW_{11}-\lambda e^{-i\theta_1} & -S\bar{W}_{1j} \\ -S\bar{W}^*_{j1} & 1-\varepsilon+SW^*_{jj}-\lambda e^{i\theta_j} \end{vmatrix} = 0 \quad (12)$$

Setting

$$\rho = \lambda e^{i(\theta_j-\theta_1)/2}, \quad \theta_{12} = (\theta_1+\theta_j)/2 \quad (13)$$

one finds, for small θ_{ij}, that the absolute value of the roots can be written as

$$|\rho| = |\lambda| \simeq 1-\epsilon+S\left(\frac{U_{11}+U_{jj}}{2}\right) \pm Re\sqrt{S^2\bar{W}_{1j}\bar{W}^*_{j1}+\left[\frac{S}{2}(U_{11}+U_{jj})+\frac{iS}{2}(V_{11}+V_{jj})+i\theta_{ij}\right]^2} \quad (14)$$

The greatest deviation from $S_{max} \simeq \varepsilon$ occurs for j=0 (corresponding to mode 60). In this case

$$\bar{W}_{10}\bar{W}^*_{01} \simeq \left(\frac{\pi^2}{8}-\frac{1}{2}-\frac{i\pi}{4}\right)^2 .$$

The maximum value of S occurs for $|\rho| = 1$, and Equation (14) leads directly to the upper curve in Figures 1,2 in region III, in agreement with the more elaborate numerical results as long as mode 60 is included. This corresponds to a resonance between the average frequency of modes 60 and 61, and the 6th harmonic of the beam bunch frequency.

Similar results apply for j=2 (region V which occurs only when mode 63 is included), and j = -1 (which occurs only when mode 59 is included, but overlaps with the resonance in region II). In these cases we use

$$U_{22} \simeq 0, \; V_{22} \simeq \frac{\pi}{8}, \; \bar{W}_{12}\bar{W}^*_{21} \simeq \left(\frac{1}{6}+i\,\frac{\pi}{8}\right)^2$$

$$U_{33} \simeq \frac{1}{27}, \; V_{33} \simeq 0, \; \bar{W}_{13}\bar{W}^*_{31} \simeq \left(\frac{\pi}{12}-\frac{i}{9}\right)^2$$

$$U_{-1-1} \simeq -1, \; V_{-1-1} \simeq 0, \; \bar{W}_{1-1}\bar{W}^*_{-1\,1} \simeq -1$$

to obtain the upper curves in the corresponding regions.

V. Conclusions

We have explored the dependence of starting current on the frequency and band width of the first transverse band in the vicinity of a resonance of the transverse mode frequencies with a multiple of the beam bunch frequency. This dependence shows unusually complex structure. However, it is possible to understand each feature of the structure in terms of a resonance with individual modes in the band or with a pair of such modes. No further complexity is expected when additional modes are considered beyond the central mode and two nearest neighbors on each side. Despite the structure, it is still true that the starting current never falls below 60% of its value for non-resonant conditions, which has formed the basis for previous estimates.

References and Footnotes

1 P. B. Wilson, HEPL Report No. 297, Stanford, June 1963; HEPL-TN-67-2, Stanford, March 1967.

2 R. L. Gluckstern and H. S. Butler, IEEE Trans. on Nuclear Science, Vol. 12N, No. 3, p. 607, June 1965.

3 Gluckstern, Butler and Jacobs, Proc. of the Vth Intl. Conf. on High Energy Accelerators, p. 649, Sept. 1965.

† Supported by the National Science Foundation.

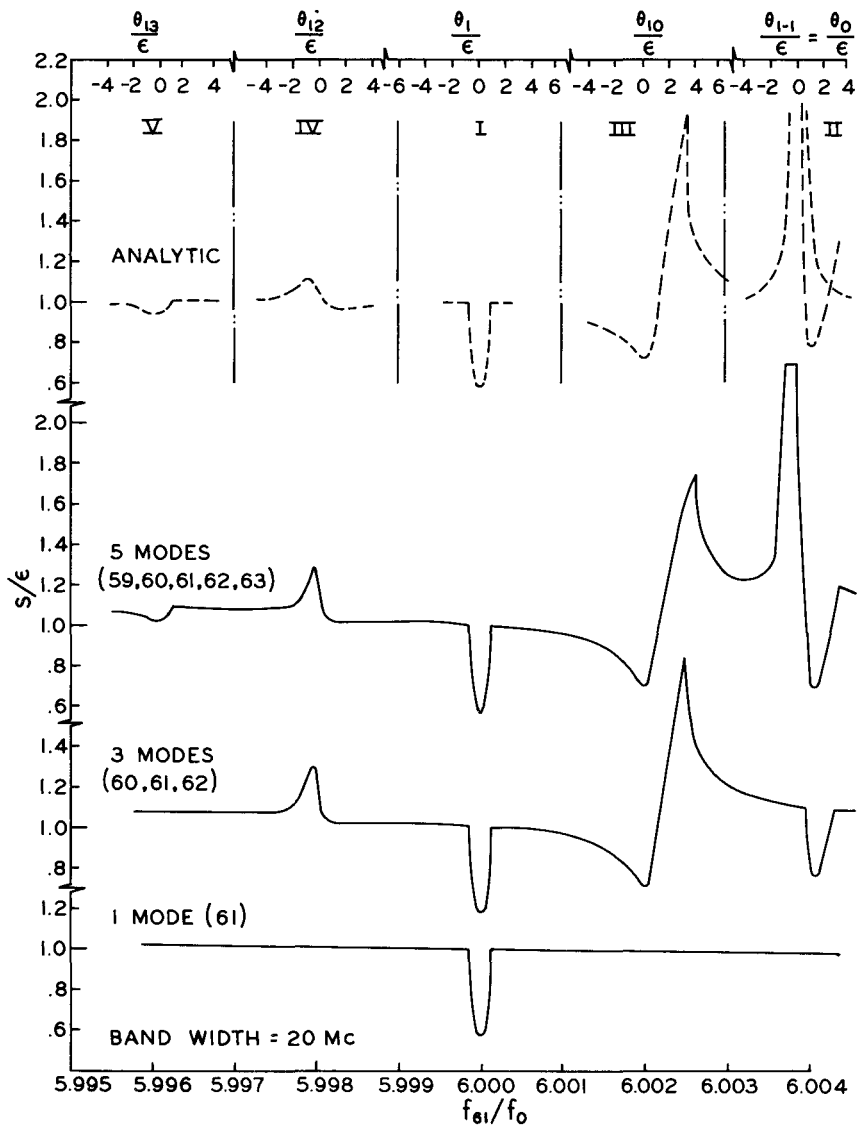

Figure 1. Starting current vs. frequency for a band width of 20 Mc. The calculations have been performed for a 40 cell tank, with the loss parameter $\epsilon = 10^{-3}$. The lowest three curves are the result of a calculation involving matrix inversion using the indicated participating modes. The upper curves represent the analytic prediction on the basis of one-and two-mode resonances with the beam frequency.

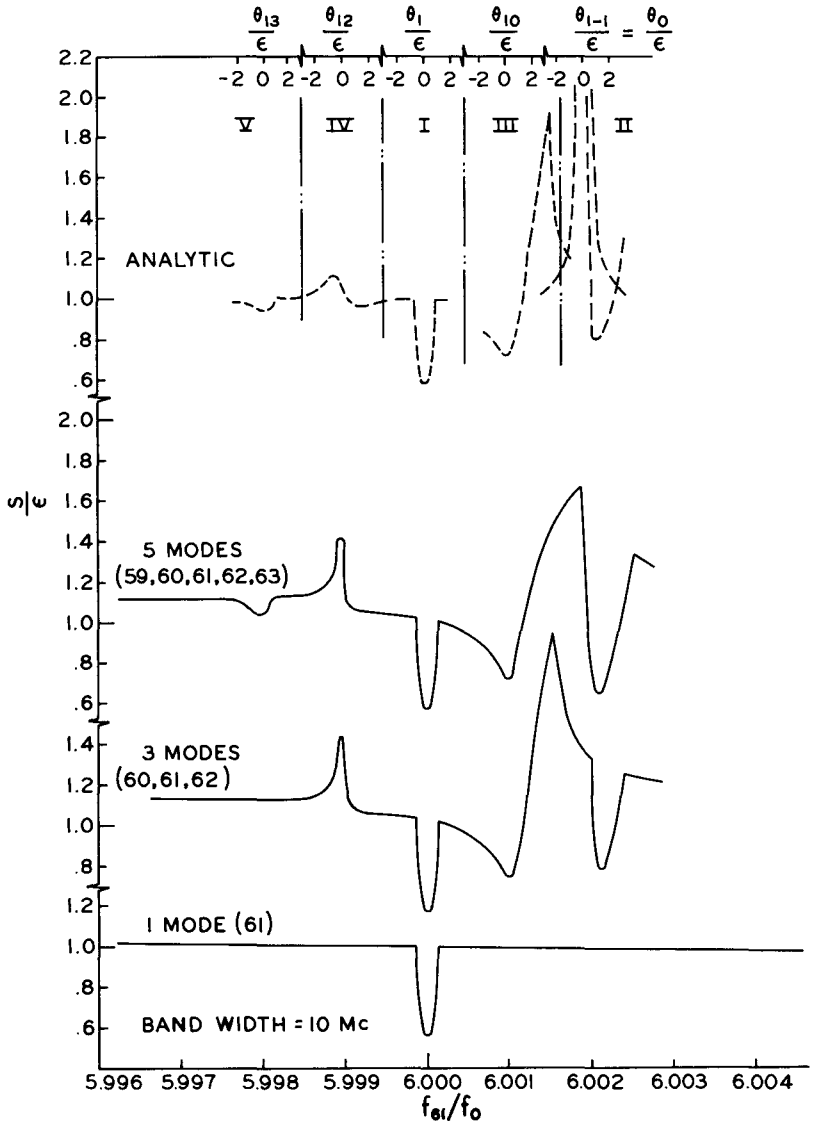

Figure 2. Starting current vs. frequency for a band width of 10 Mc. The calculations have been performed for a 40 cell tank, with the loss parameter $\epsilon = 10^{-3}$. The lowest three curves are the result of a calculation involving matrix inversion using the indicated participating modes. The upper curves represent the analytic prediction on the basis of one-and two-mode resonances with the beam frequency.